# Effect of Annealing at Temperatures Around Glass Transition Temperature on Molecular Orientation and Shrinkage of Ethylene–Vinyl Alcohol Copolymers

HIROHISA YOSHIDA, KUNIO TOMIZAWA, and YASUJI KOBAYASHI,
*Department of Industrial Chemistry, Faculty of Technology, Tokyo Metropolitan University, Setagaya-ku, Tokyo, Japan*

## Synopsis

The effect of annealing on the molecular arrangement of ethylene–vinyl alcohol copolymers (EVA) was studied by optical methods. Drawn samples were annealed at temperatures near the glass transition temperature $T_g$ in two cases; the first case allowed thermal shrinkage and the second case did not. For annealing below $T_g$, the hydroxyl groups were rearranged only to the stable position. Thermal shrinkage occurred by annealing at temperatures between $T_g$ and $T_g$ + 20–30 K. In the case of annealing at temperatures above $T_g$ + 30 K, thermal shrinkage and crystallization occurred. The crystallization by annealing made the drawn sample difficult to shrink.

## INTRODUCTION

There are two types of glassy states: one is the glass of an amorphous polymer and the other is obtained by quenching from the molten state of a crystalline polymer. Whatever the crystalline or amorphous polymer, the glassy state is influenced by its thermal history. Yeh and Geil[1,2] reported that the ball-like structure which was found in quenched poly(ethylene terephthalate) grew with annealing at a slightly lower temperature than the glass transition temperature $T_g$.

The molecular arrangement of the drawn sample is affected by annealing. If the drawn sample is kept above $T_g$, shrinkage occurs. In the case of annealing below $T_g$, shrinkage occurs only slightly because main chain motion is not possible. In contrast, the molecular arrangement of the side chains is affected by annealing below $T_g$, as the local segmental motion and the side chain motion are viable below $T_g$.

Ethylene–vinyl alcohol copolymer (EVA), which is obtained by the saponification of ethylene–vinyl acetate copolymer, consists of a hydrophobic ethylene component and a hydrophilic vinyl alcohol component. In previous studies,[3,4] the hydroxyl groups of EVA and highly saponified ethylene–vinyl acetate copolymers acted as a crosslink between molecules and affected the orientation behavior during drawing. In this paper, the effect of annealing at various temperatures on the molecular orientation of EVA is reported.

Journal of Applied Polymer Science, Vol. 24, 2277–2287 (1979)

0021-8995/79/0024-2277$01.00

## EXPERIMENTAL

### Samples

Two types of EVA were used in these experiments. The contents of vinyl alcohol in samples A and B were 68.5 and 22.0 mole %, respectively.[4] EVA was obtained by the saponification of ethylene–vinyl acetate copolymer.[5] In order to estimate the infrared dichroic ratio, thin films about 10–20 $\mu$m) were prepared. The thin films of sample B for the infrared dichroism measurement were obtained by saponification of the cast ethylene–vinyl acetate films in alkali–methyl alcohol solution (about 3 g sodium hydroxide in 350 ml methyl alcohol) at room temperature for a few weeks. The thickness of the films of sample B were about 10 $\mu$m. The termination of saponification was confirmed by infrared spectra with the disappearance of the carbonyl absorption. The saponified sample A was pressed at 468°K in a hot press and quenched in ice water. The thickness of the sample A films was about 60 $\mu$m.

### Drawing

Specimens 10 cm × 3 cm in size were cut out from the film. The specimens were drawn at the rate of 100 mm/min at 353 K. Immediately after drawing, samples were quenched in ice water and dried at 293 K for a week over phosphorus pentoxide in vacuo. During the drying, the samples were held in a holder to avoid shrinkage.

### Measurements

Infrared spectra and infrared dichroism were obtained using a Hitachi model 285 grating spectrophotometer equipped with the silver chloride polarizer. Birefringence was measured with the sodium *D* line (589 nm) using a polarized microscope equipped with a Berek compensator. Refractive index was measured using an Abbé refractometer at 298 K. Thermal analysis was carried out using a Perkin–Elmer DSC IB. Sample weight was about 5 mg. The density of the annealing sample was measured using a density gradient column prepared with carbon tetrachloride and *n*-heptane. The column temperature was 296 K. X-ray diffractograms were obtained with a Rigaku Denki model RU-3 X-ray diffractometer equipped with a proportional counter.

### Annealing

Annealing was carried out at temperatures between 323 and 393 K at 10 K intervals for various times in an air oven. Temperature was controlled within ± 0.1 K. When a sample was placed in an air oven, the controlled temperature fell momentarily. Temperature equilibration was assumed to be instantaneous. Immediately following annealing, birefringence and refractive index measurements were carried out. During the annealing, the samples were held by two different methods as described below:

**Annealing I.** Samples were held without restriction in order to permit thermal shrinkage.

**Annealing II.** Samples were mounted in an aluminum holder to avoid thermal shrinkage.

## RESULTS AND DISCUSSION

### Undrawn Samples

Both undrawn films of samples A and B show amorphous X-ray diffractograms. From thermal analysis, the glass transition temperatures of undrawn sample A and B are 331.8 and 327.6 K, respectively. The values were determined by the extrapolation of the heating velocity to zero.

### Drawn Samples

Judging from the refractive indices along three axes of drawn samples, the orientation type of drawn EVA used in this study was a cylindrical symmetric orientation. Birefringence of the drawn sample changed slightly after drying.

### Orientation Behavior

The orientation state of drawn samples can be estimated by infrared dichroism.[6–8] In the case of uniaxial drawing, the orientation factor $F_j$ can be defined[9–11] by the equation

$$F_j = \frac{D_j^0 - 1}{D_j^0 + 2} \frac{2}{3(\cos^2 \theta) - 1} \tag{1}$$

where $D_j^0$ is the dichroic ratio ($D_j^0 = (I_j^0)_\parallel / (I_j^0)_\perp$) and $\theta$ is the angle between the transition moment and the molecular axis. In the measurement of the polarized infrared spectra of drawn EVA, the normal dichroism to the drawing axis was observed at 720 $cm^{-1}$. The absorption band observed at 720 $cm^{-1}$ is assigned to the $CH_2$ rocking vibration. The absorption band at 720 $cm^{-1}$ is observed only by an incident polarized infrared beam which is parallel to the $b$ axis of polyethylene crystals.[12–14] The orientation factor $F_j$ is calculated from infrared dichroism observed at 720 $cm^{-1}$ which is the ethylene component of EVA. The transition moment of the $CH_2$ rocking vibration is perpendicular to the molecular axis; $\theta = 90°$ is therefore substituted in eq. (1). The orientation factor for the ethylene component, $F_{eth}$, was defined as follows:

$$F_{eth} = -2(D_{720}^0 - 1)/(D_{720}^0 + 2) \tag{2}$$

where $D_{720}^0$ is the infrared dichroic ratio at 720 $cm^{-1}$,

$$D_{720}^0 = (I_{720}^0)_\parallel / (I_{720}^0)_\perp \tag{3}$$

where $(I_j^0)_\parallel$ and $(I_j^0)_\perp$ are the parallel and perpendicular absorbances to the molecular axis, respectively.

Considering the additivity of birefringence, the observed birefringence $\Delta n_{total}$ can be defined by

$$\Delta n_{total} = \sum_i (\Delta n_i^0 F_i v_i) + \Delta n_{form} \tag{4}$$

where $\Delta n_i^0$, $F_i$, and $v_i$ are the intrinsic birefringence, the orientation factor, and the volume fraction of $i$th component respectively; and $\Delta n_{form}$ is the form birefringence arising from the interface between the phases. When the drawn sample

of EVA is constituted with the amorphous phase and the form birefringence is negligibly small,[15] the total birefringence can be described by the equation

$$\Delta n_{\text{total}} = \Delta n^0_{\text{eth}} F_{\text{eth}} v_{\text{eth}} + \Delta n^0_{va} F_{va} v_{va} \quad (5)$$

The intrinsic birefringence of amorphous polyethylene ($\Delta n_{\text{eth}}$) and poly(vinyl alcohol) ($\Delta n^0_{va}$) are $44 \times 10^{-3}$ and $42 \times 10^{-3}$, respectively.[16,17] The orientation factor for the ethylene component, $F_{\text{eth}}$, can be obtained by using eq. (2). The volume fraction for ethylene ($v_{\text{eth}}$) and vinyl alcohol ($v_{va}$) components are calculated from the content of vinyl alcohol in samples using the densities of polyethylene (0.925 g/cm$^3$) and poly(vinyl alcohol) (1.252 g/cm$^3$). The volume fractions for the ethylene component in samples A and B were 28 and 75 vol %, respectively. Finally, the orientation factor for the vinyl alcohol component can be obtained by using eq. (5).

The total birefringence and the orientation factors for the ethylene ($F_{\text{eth}}$) and vinyl alcohol ($F_{va}$) components in sample B are plotted as a function of the draw ratio in Figure 1. Judging from the orientation factor, the ethylene component, which was the most flexible chain in EVA, oriented selectively in the initial state of drawing. For the samples that were drawn more than four times their original length, the value of the orientation factor for the ethylene component was equal to that for perfect orientation. After most of the ethylene component, which was the flexible segment, aligned to the drawn axis, the vinyl alcohol component, which was the hard segment, began to align gradually. The orientation behavior of sample A shows the same tendency as sample B.

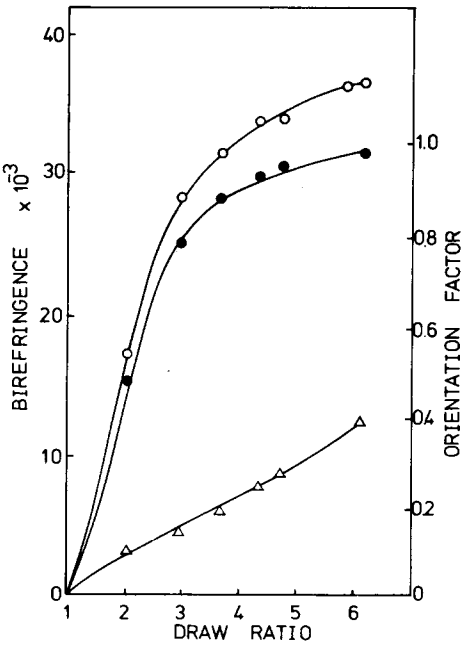


Fig. 1. Total birefringence and orientation factor changes with drawing. Vinyl alcohol content of sample is 22.0 mole % (sample B): (○) total birefringence measured by using a polarized microscope equipped with a Berek compensator; (●) orientation factor of ethylene component calculated from the infrared dichroism observed at 720 cm$^{-1}$ by using eqs. (2) and (3); (△) orientation factor of vinyl alcohol component calculated by using eq. (4).

## Effect of Annealing I

Figure 2 shows the recovery of the sample length and the birefringence of sample A with annealing I. Samples were obtained by drawing to approximately four times their original length. The recovery of the length through annealing is defined as follows:

$$\text{recovery (\%)} = (L_d - L_s)/(L_d - L_0) \times 100 \tag{6}$$

where $L_0$ is the length before drawing, $L_d$ is the length after drawing and $L_s$ is the length after annealing.

The recovery of the birefringence by annealing is defined as follows:

$$\text{recovery (\%)} = (\Delta n_d - \Delta n_s)/(\Delta n_d) \times 100 \tag{7}$$

where $\Delta n_d$ and $\Delta n_s$ are the birefringence before and after the annealing, respectively. In the case of annealing above $T_g$, thermal shrinkage occurred. However, the shrinkage hardly occurred within the experimental error by annealing below $T_g$. The higher the annealing temperature, the more the recovery of the length. In the case of annealing below 363 K, the birefringence decreased and approached a constant value. However, in the case of annealing above 373 K, the birefringence decreased in the initial period of the annealing, and then increased to saturation. Sample A used for annealing (Figs. 2–5) was obtained by drawing to four times its original length.

For the samples that were annealed for 10 min, the recovery of the birefringence was plotted as a function of the recovery of length (Fig. 3). For annealing below 363 K, a linear relationship exists between the recovery of length and birefringence. This relationship is not observed above 373 K. These facts show that the birefringence decreases as a result of thermal shrinkage in the case of annealing below 363 K. In contrast, for the annealing above 373 K, the structure changes along with the thermal shrinkage. The relationship does not extrapolate to zero, but suggests a 2% recovery of birefringence with zero length recovery (Fig. 3). It may be caused by the influence of the form birefringence arising from the interface between crystallites and amorphous regions. The values for highly drawn polyethylene were within 5% of the total birefringence.[15]

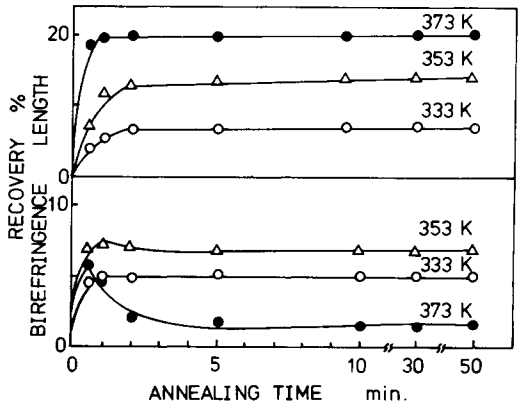


Fig. 2. Recovery of the sample length and birefringence of sample A with annealing in the case of allowing thermal shrinkage. Numbers in the figure show annealing temperatures. Recoveries are defined by eqs. (6) and (7). Samples are obtained by drawing to about four times their original length.

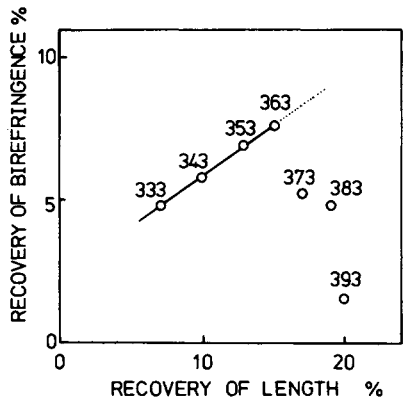


Fig. 3. Relation between the recovery of birefringence and sample length of sample A after annealing for 10 min. Numbers in the figure show annealing temperatures. In the case of annealing below 363 K, which is above $T_g$, a linear relationship between the two recoveries is found. Samples are obtained by drawing to four times their original length.

The density change with annealing I at 393 K is shown in Figure 4. Compared with the density and the birefringence, annealing causes similar changes. As the density and the birefringence increase by annealing, the annealing sample

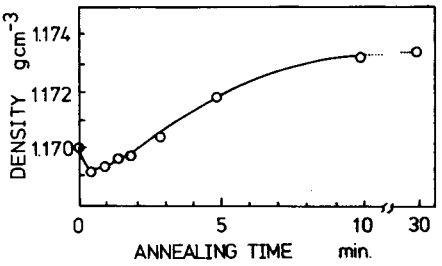


Fig. 4. Density change of sample A by annealing at 393 K in the case of allowing thermal shrinkage. Sample is obtained by drawing to four times its original length.

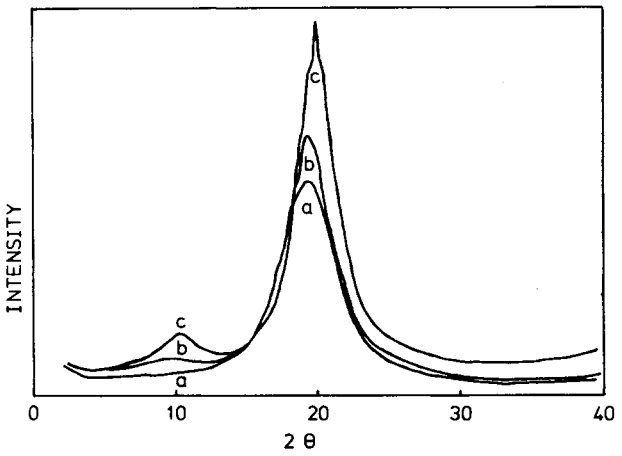


Fig. 5. X-ray diffractograms of sample A. Samples are obtained by drawing to four times their original length: (a) sample before annealing; (b) annealed sample at 363 K for 30 min; (c) annealed sample at 393 K for 30 min.

may crystallize and the crystallites may arrange parallel to the drawing direction. In order to investigate the effect of annealing above $T_g$ + 30 K, the X-ray diffractograms of sample A were prepared (Fig. 5). The drawn sample before annealing (a) shows the typical amorphous pattern; however, the annealed sample at 393 K for 30 min (c) shows the overlapping pattern of the crystal and amorphous regions. The annealed sample at 363 K for 30 min (b) shows the appearance of the ordered region. Judging from the X-ray diffractograms of the annealed sample, the increase in density is the result of the crystallization; however, it is not clear why the density decreases in the initial annealing period. For annealing above 373 K, the disappearance of the relationship between the recovery of birefringence and length (Fig. 3) is caused by the crystallization. The isothermal crystallization causes the sample to shrink slightly more than expected with the higher annealing temperature. Such self-hardening phenomena was reported for highly oriented polyethylene.[18] Judge and Stein[19] reported the growth of crystals from the molten state of crosslinked oriented polyethylene by using X-ray diffraction and optical techniques. The mechanism of cold crystallization of oriented polymers is still unknown.

## Effect of Annealing II

The changes in birefringence and the orientation factor for the ethylene component of sample B by annealing II are shown in Figure 6. Samples used for annealing were obtained by drawing to about four times their original length. In this case, the sample length never changed during annealing. The birefringence increases by annealing above $T_g$, and it increases with higher annealing

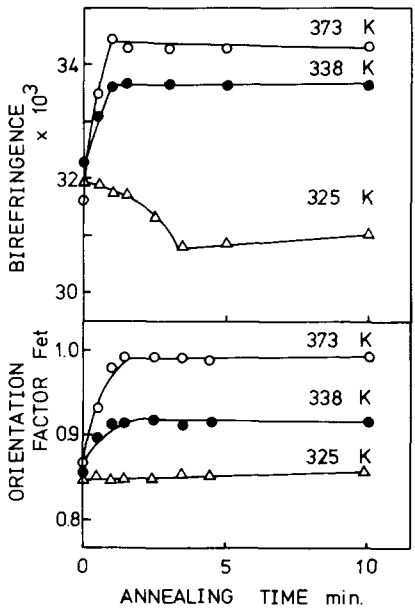


Fig. 6. Total birefringence and orientation factor of ethylene component changes with annealing in the case of sample B mounted to avoid shrinkage. Numbers in figure show annealing temperatures. Birefringence and orientation factor of ethylene component increase with annealing above $T_g$ (373 and 338 K). However, in the case of annealing below $T_g$ (325 K), birefringence decreases and the orientation factor never changes. $T_g$ of sample is 327.6 K.

temperatures. In contrast, the birefringence decreases by annealing below $T_g$. The $T_g$ of sample B was 327.6 K.

The orientation factor for the ethylene component, $F_{eth}$, scarcely changes by annealing below $T_g$ but increases by annealing above $T_g$. On the other hand, in the case of annealing at 373 K, the value of the orientation factor approaches 1. For sample A, containing more hydroxyl groups than sample B, the birefringence changes by annealing II show the same tendency as those for sample B. However, the birefringence of sample A decreases more than that of sample B by annealing below $T_g$.

In order to investigate the effect of annealing at temperatures around $T_g$, the refractive indices along three axes of drawn sample were measured. The three axes are fixed within the space of the drawn sample as shown in Figure 7. The $a$ axis is perpendicular to the film surface, the $c$ axis is parallel to the direction of drawing, and the $b$ axis is perpendicular to $a$ and $c$ axes. The variation of the refractive indices along three axes of sample A by the annealing II are shown in Figure 8. The samples used for annealing were obtained by drawing to about four times the original length. The sample was annealed at 343 K, which is above $T_g$. From the top, Figure 8 shows the refractive indices along the $a$ axis, $b$ axis, and $c$ axis, respectively. In the initial period of annealing, the refractive index along the $c$ axis increases and saturates gradually, but those along the $a$ and $b$ axes increase only slightly. Judging from the refractive indices along three axes of drawn sample and the orientation factor for the ethylene component (Fig. 6), the molecules rearrange in a parallel direction to the drawing axis. As the orientation of molecules was elevated by annealing above $T_g$, the refractive index along the $c$ axis and the birefringence increased.

The variation of the refractive indices along the three axes of sample A by annealing II at 328 K below $T_g$ are shown in Figure 9. The refractive index along the $c$ axis decreases slightly; however, those along the $a$ and $b$ axes increase slightly by annealing. These data indicate that the slight decrease in birefringence with annealing below $T_g$ is caused by the increase in the refractive indices along the $a$ and $b$ axes. The orientation of molecules along the $a$ and $b$ axes also increases.

For investigating the molecular motion of the hydroxyl groups by annealing at temperatures below $T_g$, the infrared dichroic ratio of the OH absorption band was measured. From eq. (1), the orientation function for the hydroxyl groups is defined as follows:

$$\frac{D^0_{OH} - 1}{D^0_{OH} + 2} = \frac{3\cos^2\theta_{OH} - 1}{2} F_{OH} \tag{8}$$

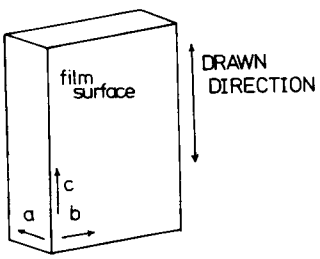


Fig. 7. Fixing of three axes within the space of drawn sample: $a$ axis is perpendicular to the film surface, $c$ axis is parallel to the direction of drawing, and $b$ axis is perpendicular to the $a$ and $c$ axes.

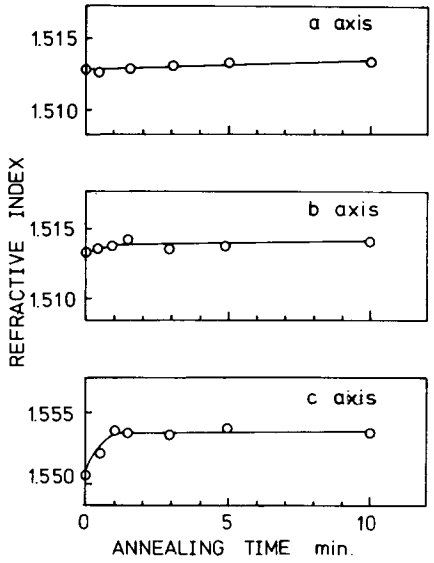


Fig. 8. Change with annealing in refractive indices along three axes of sample A in the case of the sample mounted to avoid shrinkage. From top, figures show refractive index along *a*, *b*, and *c* axes. Annealing temperature is 343 K, which is above $T_g$.

$$D^0_{\mathrm{OH}} = (I^0_{3350})_{\parallel}/(I^0_{3350})_{\perp} \tag{9}$$

where $D^0_{OH}$ is the infrared dichroic ratio at 3350 $\mathrm{cm}^{-1}$ and $F_{\mathrm{OH}}$ is the orientation factor for the hydroxyl groups. The absorption band observed at 3350 $\mathrm{cm}^{-1}$ is assigned to the OH stretching vibration. The orientation function for the hydroxyl groups, $(D^0_{3350} - 1)/D^0_{3350} + 2)$, changes with annealing II at temperature

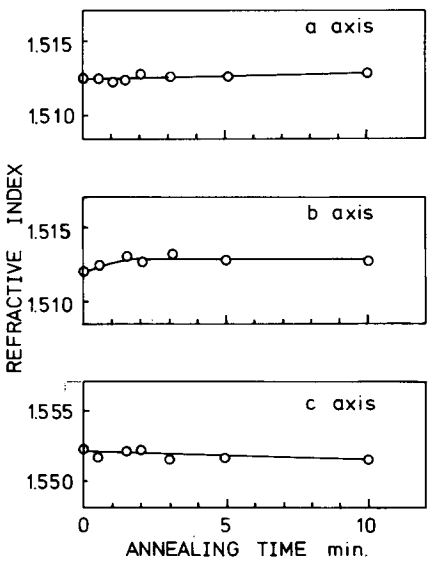


Fig. 9. Change with annealing in refractive indices along three axes of sample A in the case of the sample mounted to avoid shrinkage. From top, figures show refractive index along *a*, *b*, and *c* axes. Annealing temperature is 328 K below $T_g$.

below $T_g$ (Fig. 10). Samples were obtained by drawing to about four times their original length of sample B and annealing at 325 K. Considering the crystal structure of poly(vinyl alcohol),[20] the angle between the transition moment of the OH stretching vibration and the molecular axis, $\theta_{OH}$, is 63°. It will be assumed that the position of the hydroxyl groups in the crystal is the most stable position. As $\theta_{OH} = 63°$ is substituted in eq. (8), the orientation function for the hydroxyl groups at the stable position can be obtained. Its value is −0.190. As shown in Figure 10, the hydroxyl groups rearranged to the stable position with the annealing.

Since the segmental motion of the main chain was frozen below $T_g$ and the orientation factor for the ethylene component, which is the flexible component of EVA copolymer, hardly changed by annealing below $T_g$, the increase in refractive indices along the $a$ and $b$ axes is the result of the rearrangement of the hydroxyl groups. In general, the local molecular motion, especially the vibrational and the rotational motion of side groups, is possible below $T_g$. The glassy state of random terpolyamide was changed with the formation of hydrogen bonding[21] by annealing at slightly lower temperatures than $T_g$. For polymers containing hydroxyl groups such as EVA,[22] oligosaccharides,[23] and cellulose,[24,25] the molecular motion of the hydroxyl groups was reported at temperatures 250–320 K, which were below $T_g$. In the case of annealing below $T_g$, the rearrangement of the hydroxyl groups appears possible. Therefore, the hydroxyl groups, containing the molecular distortion which was caused by drawing, may rearrange to the stable state in order to eliminate the distortion.

## CONCLUSIONS

We propose the following interpretation of the thermal behavior of oriented EVA copolymer with annealing at various temperatures:

1. Annealing at slightly lower temperatures than $T_g$. In the temperature range from $T_g$ − 10 K to $T_g$, thermal shrinkage never occurs and the hydroxyl groups rearrange in order to eliminate the molecular distortion which was caused by drawing.

2. Annealing at slightly higher temperatures than $T_g$. In the temperature range from $T_g$ to $T_g$ + 20–30 K, thermal shrinkage occurs and there is a linear

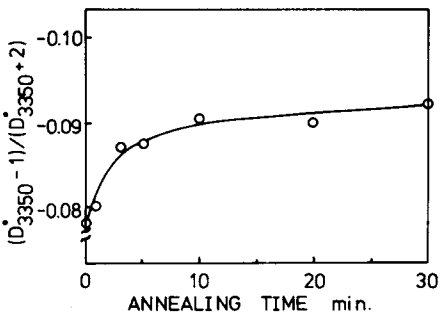


Fig. 10. Infrared orientation function of hydroxyl group change with annealing. Sample is obtained by drawing to four times its original length. Vinyl alcohol content of sample is 22.0 mole % (sample B). Orientation function, which is defined by eq. (8), is the function of orientation factor of hydroxyl group.

relationship between the recovery of length and birefringence. For the sample which was mounted in a holder so as not to shrink, the most flexible part of the copolymer was drawn by the force which was produced by the thermal shrinkage.

3. Annealing at higher temperatures than $T_g$. EVA copolymer crystallizes isothermally by annealing above $T_g + 30$ K. Crystallization causes the hardening of the drawn sample, and the sample barely shrinks.

Molecular motion of hydroxyl groups below $T_g$ and the self-hardening mechanism for drawn samples by annealing above $T_g$ should be examined further.

## References

1. G. S. Y. Yeh and P. H. Geil, *J. Macromol. Sci., Phys.*, **1**, 235 (1967).
2. G. S. Y. Yeh and P. H. Geil, *J. Macromol. Sci., Phys.*, **1**, 251 (1967).
3. H. Yoshida and Y. Kobayashi, *Rep. Progr. Polym. Phys. Jpn.*, **20**, 409 (1977).
4. H. Yoshida and Y. Kobayashi, *Sen-i Gakkaishi (J. Soc. Fiber Sci. Technol. Jpn.)*, **33**, T-479 (1977).
5. T. Matsumoto et al., *Kobunshi Kagaku (J. Soc. Polym. Chem. Jpn.)*, **28**, 610 (1971).
6. R. Zbinden, *Infrared Spectroscopy of High Polymers*, Academic Press, New York, 1964, p. 225.
7. R. J. Samuels, *J. Polym. Sci., Part A-1*, **3**, 1741 (1965).
8. Y. Kobayashi, S. Okajima and A. Narita, *J. Appl. Polym. Sci.*, **11**, 2515 (1967).
9. R. S. Stein and F. H. Norris, *J. Polym. Sci.*, **21**, 381 (1956).
10. R. S. Stein, *J. Polym. Sci.*, **31**, 327 (1958).
11. R. S. Stein, *J. Polym. Sci.*, **50**, 339 (1961).
12. R. S. Krimm, *J. Chem. Phys.*, **22**, 567 (1954).
13. A. Keller and I. Sanderman, *J. Polym. Sci.*, **15**, 133 (1955).
14. R. S. Stein, *J. Chem. Phys.*, **23**, 734 (1955).
15. F. A. Bettelheim and R. S. Stein, *J. Polym. Sci.*, **27**, 567 (1958).
16. C. W. Bunn and E. V. Garner, *Proc. Royal Soc., London, Ser. A*, **189**, 39 (1947).
17. S. Okajima and Y. Kobayashi, *Kogyo Kagaku Zasshi (J. Chem. Soc. Jpn., Ind. Chem. Sect.)*, **59**, 82 (1956).
18. R. G. C. Arridge, P. J. Barham, and A. Keller, *J. Polym. Sci., Polym. Phys. Ed.*, **15**, 389 (1977).
19. J. T. Judge and R. S. Stein, *J. Appl. Phys.*, **32**, 2357 (1961).
20. C. W. Bunn, *Nature*, **161**, 929 (1948).
21. T. Hatakeyama and H. Kanetsuna, *J. Polym. Sci., Polym. Phys. Ed.*, **11**, 815 (1973).
22. H. Yoshida, K. Tomizawa, and Y. Kobayashi, *Rep. Progr. Polym. Phys. Jpn.*, **21**, 201 (1978).
23. M. V. Ramiah and D. A. I. Goring, *J. Polym. Sci., Part C*, **11**, 27 (1965).
24. I. Kubat and C. Pattyranie, *Nature*, **215**, 390 (1967).
25. S. Yano, H. Hatakeyama, and T. Hatakeyama, *J. Appl. Polym. Sci.*, **20**, 3221 (1976).

Received November 29, 1978
Revised June 29, 1979